

# Postmortem Autopsy-Confirmation of Antemortem [F-18]FDDNP-PET Scans in a Football Player With Chronic Traumatic Encephalopathy

Bennet Omalu, MD, MBA,  
MPH\*

Gary W. Small, MD<sup>‡</sup>

Julian Bailes, MD<sup>§</sup>

Linda M. Ercoli, PhD<sup>‡</sup>

David A. Merrill, MD, PhD<sup>‡</sup>

Koon-Pong Wong, PhD<sup>¶</sup>

Sung-Cheng Huang, DSc<sup>¶</sup>

Nagichettiar Satyamurthy,  
PhD<sup>¶</sup>

Jennifer L. Hammers, DO<sup>||</sup>

John Lee, MD, PhD<sup>#</sup>

Robert P. Fitzsimmons, JD\*\*

Jorge R. Barrio, PhD<sup>¶</sup>

\*Department of Medical Pathology and Laboratory Medicine, School of Medicine, University of California, Davis, Sacramento, California; <sup>‡</sup>Department of Psychiatry and Biobehavioral Sciences, Semel Institute for Neuroscience and Human Behavior, The David Geffen School of Medicine, University of California, Los Angeles, California; <sup>§</sup>Department of Neurosurgery, North Shore University Health System and University of Chicago Pritzker School of Medicine, Evanston, Illinois; <sup>¶</sup>Department of Molecular and Medical Pharmacology, The David Geffen School of Medicine, University of California, Los Angeles, California; <sup>||</sup>Office of Chief Medical Examiner, City of New York, New York; <sup>#</sup>Department of Pathology, North Shore University Health System and University of Chicago Pritzker School of Medicine, Evanston, Illinois; \*\*Fitzsimmons Law Firm PLLC, Wheeling, West Virginia

## Correspondence:

Bennet Omalu, MD, MBA, MPH,  
8150 Scenic Trails Way,  
Sacramento, CA 95829.  
E-mail: [bennetomaluu@bennetomaluu.com](mailto:bennetomaluu@bennetomaluu.com)

Received, April 28, 2017.

Accepted, September 26, 2017.

Copyright © 2017 by the  
Congress of Neurological Surgeons

Currently, only presumptive diagnosis of chronic traumatic encephalopathy (CTE) can be made in living patients. We present a modality that may be instrumental to the definitive diagnosis of CTE in living patients based on brain autopsy confirmation of [F-18]FDDNP-PET findings in an American football player with CTE. [F-18]FDDNP-PET imaging was performed 52 mo before the subject's death. Relative distribution volume parametric images and binding values were determined for cortical and subcortical regions of interest. Upon death, the brain was examined to identify the topographic distribution of neurodegenerative changes. Correlation between neuropathology and [F-18]FDDNP-PET binding patterns was performed using Spearman rank-order correlation. Mood, behavioral, motor, and cognitive changes were consistent with chronic traumatic myeloencephalopathy with a 22-yr lifetime risk exposure to American football. There were tau, amyloid, and TDP-43 neuropathological substrates in the brain with a differential topographically selective distribution. [F-18]FDDNP-PET binding levels correlated with brain tau deposition ( $r_s = 0.59$ ,  $P = .02$ ), with highest relative distribution volumes in the parasagittal and paraventricular regions of the brain and the brain stem. No correlation with amyloid or TDP-43 deposition was observed. [F-18]FDDNP-PET signals may be consistent with neuropathological patterns of tau deposition in CTE, involving areas that receive the maximal shearing, angular-rotational acceleration-deceleration forces in American football players, consistent with distinctive and differential topographic vulnerability and selectivity of CTE beyond brain cortices, also involving midbrain and limbic areas. Future studies are warranted to determine whether differential and selective [F-18]FDDNP-PET may be useful in establishing a diagnosis of CTE in at-risk patients.

**KEY WORDS:** Antemortem, Autopsy, CTE, [F-18]FDDNP-PET, Football player

*Neurosurgery* 0:1–10, 2017

DOI:10.1093/neuros/nyx536

[www.neurosurgery-online.com](http://www.neurosurgery-online.com)

**W**e have reported that 2-(1-{6-[(2-[F-18]fluoroethyl)(methyl)amino]-2-naphthyl}ethylidene)malononitrile ([F-18]FDDNP) has a high affinity for  $\beta$ -pleated sheet fibrillar neuroaggregates,

which provide a high binding potential for in vivo imaging visualization of tau and amyloid fibrils.<sup>1-3</sup> We previously reported unique [F-18]FDDNP-PET patterns in the brains of 5 National Football League (NFL) players with suspected chronic traumatic encephalopathy (CTE).<sup>4</sup> We further characterized and reported the in vivo [F-18]FDDNP patterns and selective topographic distributions of CTE neuropathology in the living brains of 14 retired NFL players and compared the distinctive CTE patterns to those of 28 cognitively intact controls and 24 Alzheimer's disease patients.<sup>1</sup> CTE, like other brain diseases, exhibits selective topographic vulnerability<sup>5</sup> that progresses to involve more regions of the brain in diffuse and global patterns<sup>1</sup> as the

**ABBREVIATIONS:** CD-68, cluster of differentiation 68; CERAD, Consortium to Establish a Registry for Alzheimer's Disease; CTE, chronic traumatic encephalopathy; CTME, chronic traumatic myeloencephalopathy; DVR, distribution volume ratio; GFAP, glial fibrillary acidic protein; H/E, hematoxylin and eosin; LFB-CV, luxol fast blue-cresyl violet; MRI, magnetic resonance imaging; NFL, National Football League; ROIs, regions of interest

**Neurosurgery Speaks!** Audio abstracts available for this article at [www.neurosurgery-online.com](http://www.neurosurgery-online.com).

**TABLE 1. Major Milestones and Events in the Football History and Work History of Our Patient**

1.	Played football from 11 to 33 yr old; cumulative lifetime risk exposure of 22 yr.
	a. Youth football: 2 yr.
	b. High school football: 4 yr.
	c. College football (defensive end): 4 yr.
	d. Professional football (NFL-linebacker): 12 yr.
	e. Number of "bell rung" suffered: few (college and NFL football).
	f. Number of reported concussions: 1 (college football: suffered dizziness for 3 d).
2.	Graduated from college (Bachelor of Arts in Economics) before playing in the NFL.
3.	Began attending law school in 12th NFL year.
4.	Graduated from law school (Juris Doctorate) 2 yr after retirement from the NFL.
5.	Practiced law in a law firm, moved to another law firm, became partner.
	a. Dismissed as partner 3-4 yr later for lack of performance.
6.	Became a sole practitioner, relocated to another state, passed another bar examination.
7.	Worked in a new law firm, was later dismissed for lack of performance.
8.	Worked in another law firm, was later dismissed, pattern continued.
9.	Stopped practicing law 25 yr after retirement from the NFL.
10.	Socioeconomic status deteriorated progressively, filed for bankruptcy.

Our patient had a 22-yr cumulative lifetime risk exposure to football and manifested a progressive decline in his work status and performance over decades, which eventually resulted in a bankruptcy.

disease advances. The ability to identify CTE in the brains of living patients is a prerequisite step for complete elucidation of CTE pathogenesis and development of cures.<sup>6</sup> In pursuit of this prerequisite step, we present an autopsy confirmation in a retired NFL player with CTE, who had an antemortem [F-18]FDDNP-PET scan with a distinctive CTE pattern.

## METHODS

### Medical History

Our patient's medical, football, and work histories were collated and reviewed. A postmortem surrogate interview of his wife and next-of-kin was performed. He was a 59-yr-old African-American man at the time of [F-18]FDDNP-PET scanning. The magnetic resonance imaging (MRI) scan at the time of the [F-18]FDDNP-PET imaging showed mild, global brain atrophy with enlarged ventricles, moderate bilateral hippocampal atrophy, and diffuse white matter hyperintensities.

Two years after his [F-18]FDDNP-PET scan, at age 61, his wife noticed progressive motor deficits, including inability to button his shirts, zip his pants or tie his shoes, and eventually feed himself. She reported that he developed muscle twitching (without cramps) in his arms and decreased muscle mass in his shoulders and arms without any sensory changes. Clinical examinations about 6 to 8 mo after the onset of his motor symptoms revealed decreased muscle bulk in the bilateral upper extremities with normal tone, atrophy of the intrinsic hand muscles, and weakness of the biceps bilaterally. Electromyography determinations of selected bilateral upper and lower extremity, and cervical-lumbar paraspinal muscles revealed active and chronic denervation changes in nearly all muscles tested. Approximately 17 mo prior to death, he was diagnosed with Motor Neuron Disease/Amyotrophic Lateral Sclerosis in addition to his pre-existing clinical and presumptive diagnosis of CTE.

During the final months of his life, our patient was admitted to a nursing home for dehydration, failure to thrive, progressive dysphagia, incontinence, progressive neck and limb weakness, and slurred speech. He eventually died at the age of 63. Full autopsy was not performed, but his brain and spinal cord were harvested for neuropathological examination.

Neuropsychological evaluation of the patient was performed at the time of [F-18]FDDNP-PET scanning.<sup>7,8</sup>

### Antemortem [F-18]FDDNP-PET Brain Scan

[F-18]FDDNP-PET imaging of the brain was performed approximately 52 mo prior to death. The study was performed under standard ethics guidelines as have been previously reported.<sup>4</sup>

[F-18]FDDNP radiochemistry has been previously described and reported.<sup>1,4,9,10</sup> PET scan determinations and quantification of the [F-18]FDDNP binding data have been previously reported.<sup>1,4,11-13</sup> The distribution volume ratio (DVR) parametric images were generated and analyzed with the use of regions of interest (ROIs) drawn bilaterally on the co-registered MRI scans for a number of cortical, limbic, and subcortical areas. MRI scans were also performed for the purpose of anatomical reference to aid the analysis of PET data as described previously.<sup>11</sup>

### Postmortem Autopsy Determination

Upon the subject's death, the next-of-kin contacted the pathologist (BO) for donation of the patient's brain. An informed consent form was signed for brain examination and to obtain the medical records for review. The dura mater, brain, pituitary gland, and spinal cord were harvested within 48 h of death, and fixed in 10% buffered formaldehyde for 3 wk. The sections were then washed for 24 h in a water bath, measured, grossed, and dissected.

**TABLE 2. Summary of Symptoms Reported by Our Patient's Wife and Next-of-Kin at the Time of his [F-18]-FDDNP-PET Scanning**

1.	Difficulty recalling names of familiar people and recent past events.
2.	Problems with tracking conversations.
3.	Began losing personal objects.
4.	Became short-tempered, often felt panicked, was less organized.
5.	Became fixated on ideas and less interested in activities he previously enjoyed.
6.	Transformed from a kind, mild-mannered "gentle giant" to a very agitated person. a. Exhibited angry outbursts that were out of character.
7.	Behaved inappropriately as if "his filter was gone."
8.	Evaluated by a psychiatrist, diagnosed with depression, and "probable CTE."

Our patient exhibited negative family history for dementia or major psychiatric illness. According to his wife and next-of-kin, he exhibited progressive cognitive decline for many years after retirement from the NFL.

**TABLE 3. Results of Cognitive Appraisal at the Time of [F-18]FDDNP-PET Scan**

No.	Type of appraisal	Results
1.	Gross cognitive functioning	Mini-Mental State Examination: 25 out of 30.
2.	Intellectual functioning	Average range—Wechsler Test of Adult Reading (estimate of premorbid general intellectual functioning; 30th percentile, estimated FIQ = 92).
3.	Attention/Concentration	Impaired range—WAIS-III Digit Span (ninth percentile); able to recite 7 digits forward and 3 digits backward.
4.	Psychomotor/Information processing speed	Low average to impaired range—WAIS-III Digit Symbol Coding (copying symbols to match a set; 16th percentile). Stroop B (rapid word reading; fifth percentile). Stroop A (rapid color reading; second percentile). Tails A (drawing lines to connect a series of numbers; <first percentile).
5.	Language	Average to impaired range—CFL (phonetic fluency; 33rd percentile). Animals (semantic fluency; ninth percentile). Boston Naming (confrontation naming; <first percentile).
6.	Visual-spatial functioning	Average range—WAIS-III Block Design (50th percentile). Rey-O Copy, 32/36 (46th percentile).
7.	Executive functioning	Average to impaired range—WAIS-III Similarities (verbal abstract reasoning; 63rd percentile). WCST (flexibility and concept formation: completed 6/6 categories (16th percentile with several errors; 32nd percentile) Animals (semantic fluency; ninth percentile). Trails B (set-shifting; fifth percentile). Stroop C (inhibiting automatic responses; first percentile).
8.	Memory	Immediate memory: impaired range (WMS-III Verbal Pairs I: 25th percentile; WMS-III Logical Memory I: first percentile; Buschke Total: <first percentile). Delayed memory: impaired range (WMS-III Verbal Pairs II: ninth percentile; WMS-III Logical Memory II: fifth percentile; Buschke Delay: <first percentile).
9.	Hamilton Depression Rating (17-item)	8
10.	Hamilton Anxiety Scale	13

Comprehensive psychopathological cognitive assessment of the patient at the time of the [F-18]FDDNP-PET scan for the in vivo detection of neuropathological substrates in the brain. Our subject was diagnosed with mild cognitive impairment with deficits in multiple cognitive domains, eg, memory, attention, information processing speed, language, and executive functioning.

MRI/PET maps and regions of interest were used for the determination of DVR values. Similar regions of interest matching the MRI/PET maps were targeted in the neuropathological tissue sectioning and microscopic examination. A battery of histochemical and immunohistochemical stains was performed on each submitted section in addition

to routine hematoxylin and eosin (H/E). The brain slides were independently examined microscopically by 2 neuropathologists (BO and JL) and 1 forensic pathologist (JH). All 3 pathologists were in agreement with the findings and diagnoses. Histomorphological, proteinopathic, and neuroinflammatory changes were noted on all stained slides. The

**TABLE 4. Summary of Pertinent Gross and Hematoxylin and Eosin Histomorphologic Findings in the Brain and Spinal Cord**

1.	No fibrocystic membrane or xanthochromia in dura mater.
2.	Mild, diffuse, symmetrical cortical atrophy, cerebral and cerebellar hemispheres.
3.	No remote contusional necrosis of brain.
4.	Moderate, symmetrical, bilateral dilatation of all ventricles.
5.	Cavum septum pellucidum, present, without fenestrations of the septum pellucidum.
6.	Mild, bilateral, symmetrical atrophy of the cornu ammonis.
7.	No segmental necrosis or atrophy of spinal medulla.
8.	Multifocal sparse perivascular hemosiderin-laden histiocytes, Virchow Robin spaces.
9.	Diffuse, mild, neuronal loss, neocortex, subcortical nuclei, and cerebellar cortex.
10.	Severe loss of pyramidal neurons, Sommer's sector.
11.	No granulo vacuolar neuronal degeneration or Hirano bodies in stratum pyramidale.
12.	No necrosis or degeneration of the anterior, lateral, and posterior spinal funiculi.
13.	Mild neuronal loss, cervical, thoracic, and lumbar spinal medulla.

Gross and histologic (hematoxylin and eosin) examination of the brain and spinal cord revealed nonspecific findings without any focal parenchymal contusional necrosis.

distribution and density of the proteinopathic changes were classified into 4 semiquantitative categories adapted from the neuritic plaque density assessment of the Consortium to Establish a Registry for Alzheimer's Disease (CERAD).<sup>14</sup> The 4 adapted categories are as follows: none (0), sparse (1), moderate (2), and frequent (3). The same categorization was applied to pathological changes seen on the cluster of differentiation 68 (CD-68), glial fibrillary acidic protein (GFAP), and luxol fast blue-cresyl violet (LFB-CV) stains.

### Statistical Analysis

Topographic distribution of observed proteinopathies in the brain was compared to the documented topographic distribution of the [F-18]FDDNP-PET brain imaging findings. Correlation analysis was performed using Spearman rank-order correlation. Correlation between [F-18]FDDNP-PET DVRs and tau, amyloid, or TDP-43 deposit densities, was obtained and was corrected for multiple comparisons using the Benjamini-Hochberg method<sup>15</sup> and controlled the false discovery rate (FDR) to be 10%. Statistical significance was set at  $P < .05$  (2-sided). Statistical analysis was performed using the SAS 9.4 for Windows (SAS Institute Inc, Cary, North Carolina).

## RESULTS

Summaries of our patient's football, work, and medical histories are presented in Tables 1-3.

### Brain and Spinal Gross and Histologic Findings

The gross and H/E brain and spinal findings are summarized in Table 4. The LFB-CV stains revealed diffuse, global, mild loss of myelin in the cortical and subcortical white matter including the corpus callosum (Table 5). The Bielschowsky silver stains highlighted the tau and amyloid neuropathological substrates described below.

The tau immunostains revealed sparse to frequent neuronal and glial fibrillary tangles and inclusions, neuropil threads and dot-like lesions, and ghost neurofibrillary tangles, which were

differentially and topographically distributed in both the brain and spinal cord (Table 5). All these tau neuropathological substrates, in both the gray and white matter, were included in the semiquantitative evaluation of topographic densities, and were not limited to neuronal neurofibrillary tangles. In the spinal cord, the neurons, glia, and neuropil of both the central gray matter and the anterior, lateral, and posterior funiculi were involved by tau neuropathological substrates. The following diagnostic CTE criteria were noted: residual density accentuations of tauopathy in the superficial cortical laminae, in the depths of the sulci, in perivascular regions, and in the subcortical parasagittal and periventricular nuclei, as well as irregular neocortical distributions of tau neuropathological substrates (skip-phenomenon), whereby adjacent regions of the neocortex were skipped by tau substrates.<sup>16,17</sup> The parasagittal and paraventricular density-accentuations of tau substrates exhibited a caudal-rostral gradient with highest densities seen in the regions of the brain surrounding the third ventricle and cerebral aqueduct of Sylvius including the periaqueductal and tegmental nuclei of the midbrain and rostral pons, and the locus ceruleus, the hypothalamus, subthalamic nucleus, periventricular posterior thalamus and pulvinar, and the globus pallidus.<sup>16,17</sup> These subcortical regions, similar to the neocortex, exhibited the skip-phenomenon. These parasagittal and periventricular subcortical regions, with less volume and less surface area when compared to the global neocortex, appeared to show more frequent densities of tau neuropathological substrates per unit surface area and volume, with prominent extra-neuronal tau substrates, in agreement with [F-18]FDDNP-PET findings (Figures 1 and 2; Table 5). Thorn-shaped astrocytes and features of primary age-related tauopathy or age-related tau astrogliopathy were absent.<sup>18,19</sup>

The beta-A4 amyloid immunostains revealed diffuse and neuritic amyloid plaques that exhibited differential topographic distribution as shown in Table 5. There was no cerebral amyloid angiopathy in the brain or spinal cord. The amygdala, cerebellum, and spinal cord did not show any diffuse or neuritic amyloid

**TABLE 5. Semiquantitative Differential and Topographically Selective Distribution of Neurodegenerative Changes in the Brain of Our Subject**

#	Region of interest	Tau	Amyloid	A-SN	CD-68	GFAP	Ubi	TDP-43	FUS	LFB
1.	Frontal lobe, right and left	3+	3+	0	3+	3+	0	0	0	1+
2.	Temporal lobe, right and left	3+	3+	0	3+	3+	0	0	0	1+
3.	Parietal lobe, right and left	3+	3+	0	3+	3+	0	0	0	1+
4.	Occipital lobe, right and left	1+	2+	0	3+	3+	0	0	0	1+
9.	Hippocampus, right and left	3+	2+	0	3+	3+	0	0	0	1+
5.	Pulvinar/posterior thalamus, right and left	3+	1+	0	3+	3+	0	0	0	1+
6.	Cingulate gyrus, corpus callosum, and caudate nucleus, right and left	3+	2+	0	3+	3+	0	0	0	1+
7.	Amygdala, right and left, with entorhinal cortex	3+	1+	0	3+	3+	0	1+	0	1+
8.	Insula cortex, right and left	3+	3+	0	3+	3+	0	0	0	–
	Putamen, right and left	3+	1+	0	3+	3+	0	0	0	–
	Globus pallidus, right and left	3+	1+	0	3+	3+	0	0	0	–
	Internal, external, and extreme capsules, right and left	3+	0	0	3+	3+	0	0	0	1+
9.	Splenium of the corpus callosum	2+	0	0	3+	3+	0	0	0	1+
10.	Motor cortex, right and left	3+	2+	0	3+	3+	0	0	0	1+
11.	Prefrontal lobe, right and left	3+	3+	0	3+	3+	0	0	0	1+
12.	Midbrain, rostral and caudal	3+	1+	0	3+	3+	0	2+	0	1+
	Hypothalamus	3+	1+	0	3+	3+	0	2+	0	1+
13.	Pons, tegmental nuclei, rostral and caudal	3+	1+	0	3+	3+	0	0	0	1+
	Pontine nuclei and basis pontis, rostral and caudal	1+	0	0	3+	2+	0	0	0	1+
14.	Medulla oblongata, rostral and caudal	2+	0	0	3+	2+	0	0	0	1+
15.	Medulla oblongata, caudal	2+	0	0	3+	2+	0	0	0	1+
16.	Cerebellum, cortex, right and left	0	0	0	1+	3+	0	0	0	1+
	Dentate nucleus and subcortical nuclei, right and left	2+	0	0	3+	3+	0	0	0	1+
17.	Spinal cord, cervical	2+	0	0	3+	1+	0	0	0	1+
18.	Spinal cord, thoracic	2+	0	0	3+	1+	0	0	0	1+
19.	Spinal cord, lumbar	2+	0	0	3+	1+	0	1+	0	1+

CERAD-based semiquantitative differential and topographically selective distribution of inflammatory changes and neuropathological substrates in the brain of our patient. He had received an antemortem [F-18]FDDNP-PET scan 52 mo prior to his death.

Tau, PHF-tau; Amyloid, beta-A4 amyloid; A-SN, alpha-synuclein; GFAP, glial fibrillary acidic protein; Ubi, ubiquitin; TDP-43, TAR DNA-binding protein 43; FUS, fused in sarcoma protein; LFB, luxol fast blue-cresyl violet. The density of pathology and proteinopathy: 0: None; 1: Sparse; 2: Moderate; 3: Frequent.

plaques. The brainstem showed none to sparse diffuse and neuritic amyloid plaques.

The TDP-43 immunostains revealed inclusions in neurons and glia, and neuropil threads in selective regions of the brain and spinal medulla (Table 5). The alpha-synuclein, ubiquitin, and FUS protein immunostains did not reveal any neuronal or glial inclusions. The CD-68 immunostains showed diffuse, global neuropil histiocytes and activated microglia accentuated perivascularly and in the Virchow Robin spaces. The GFAP immunostains exhibited a similar topographic distribution with diffuse, global isomorphic fibrillary astrogliosis (Table 5).

The regions of the brain with the highest densities of tau pathology showed larger numbers of ghost tangles. Every region of the brain that exhibited amyloid pathology also exhibited the presence of tau pathology in higher densities; however, not every region of the brain that exhibited tau pathology, exhibited corresponding amyloid pathology. The parasagittal and paraventricular subcortical regions showed higher predominance of tau pathology compared to amyloid pathology. Brain ROIs with the highest densities of tau pathology also generally showed TDP-43

pathology deposition, typically subcortical structures (Table 5). There was no amyloid or tau pathology in the cerebellum.

The clinical and pathological findings, in this case, were consistent with a primary diagnosis of chronic traumatic myeloencephalopathy (CTME), as has been previously described.<sup>16,17,20-24</sup> Figure 3 illustrates the pertinent neuropathological findings.

### Comparison of Postmortem Neuropathological Findings with Antemortem [F-18]FDDNP-PET Imaging Results

Neuropathological findings showed indicators of the differential neocortical densities and distributions of tau neuropathological substrates identified by [F-18]FDDNP-PET brain imaging, which showed higher neocortical DVR values for the frontal and temporal cortex, lower DVR values for the parietal cortex, and lowest DVR values for the occipital cortex, in an anteroposterior gradient (Figure 1).<sup>1</sup> [F-18]FDDNP-PET identified tau pathology in the regions of the brain confirmed by

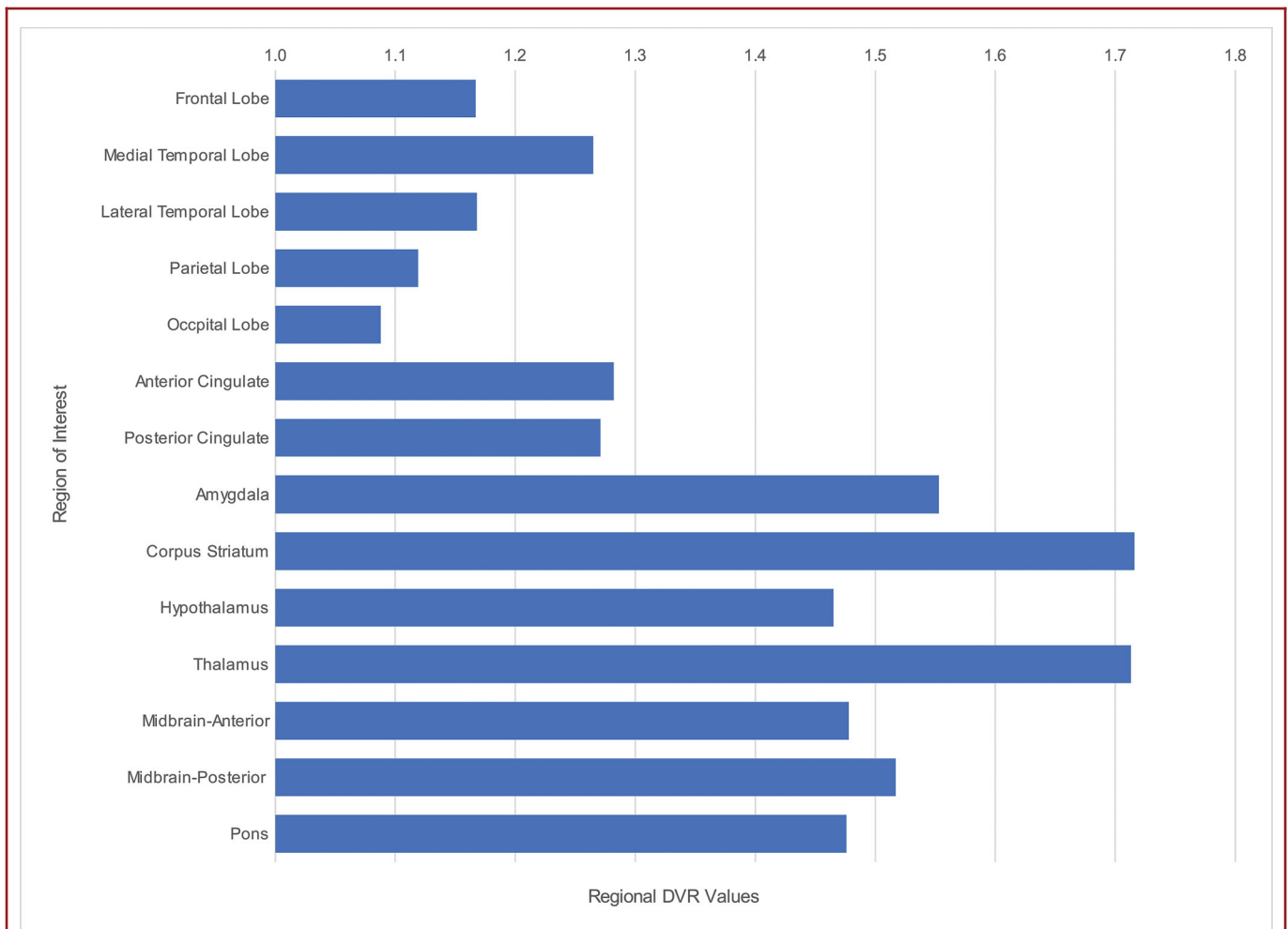


**FIGURE 1.** Bar chart illustrating the differential regional [F-18]FDDNP-PET DVR values with highest values noted in parasagittal and sagittal periventricular regions of the brain including the subcortical ganglia, amygdala, and midbrain. Note also the highest brain signals in the medial temporal and frontal lobes.

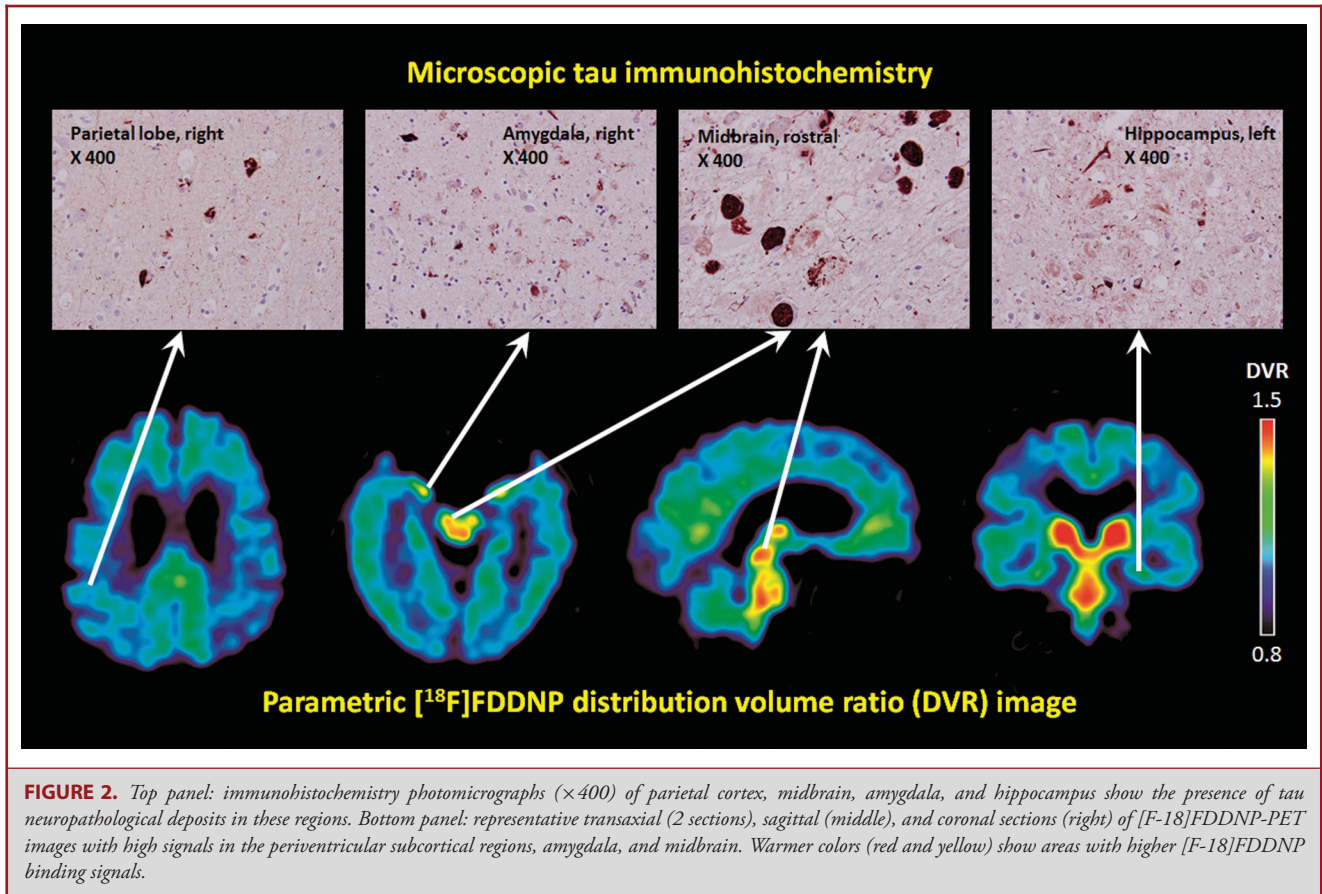
tissue analysis to show tau pathology, and also amyloid pathology in some instances; and identified regions of the brain with only tau pathology or predominant tau pathology such as the midbrain and amygdala.

Correlation analysis was performed to investigate whether the in vivo regional [F-18]FDDNP binding level agreed with the density of tau pathology based on autopsy findings. Spearman rank-order correlation coefficient ( $r_s$ ) was calculated for the regional [F-18]FDDNP DVRs (Figure 1) and the density of tau pathology, as well as for amyloid and TDP-43 substrates (Table 5). Our results showed that the tau regional findings and densities obtained from antemortem [F-18]FDDNP-PET imaging and postmortem autopsy were highly correlated ( $r_s = 0.592$ ,  $P = .0202$ ). However, no statistical correlation was found with the presence of amyloid deposition ( $r_s = -0.481$ ;  $P = .0695$ ) or of TDP-43 ( $r_s = 0.433$ ;  $P = .1066$ ).

## DISCUSSION

Our findings and previously reported research<sup>1,4,25</sup> may confirm that [F-18]FDDNP-PET brain imaging may be selective for predominant tauopathies like CTE and may identify the distinctive selective topographic differential distribution of brain tau pathology. The neuropathological findings, at brain autopsy in this current research, confirmed the in vivo [F-18]FDDNP-PET ‘fingerprint’ signature of CTE previously reported.<sup>1,4</sup>

CTE has been confirmed to exhibit a distinctive neuropathological signature with differential and selective topographic vulnerability of brain regions, which are temporally progressive<sup>1,17,20-22,26,27</sup> eventually recruiting all regions of the brain in advanced CTE.<sup>20,22</sup> The [F-18]FDDNP-PET brain imaging findings<sup>1,4</sup> and brain autopsy findings in this current research may further confirm this neuropathological signature.

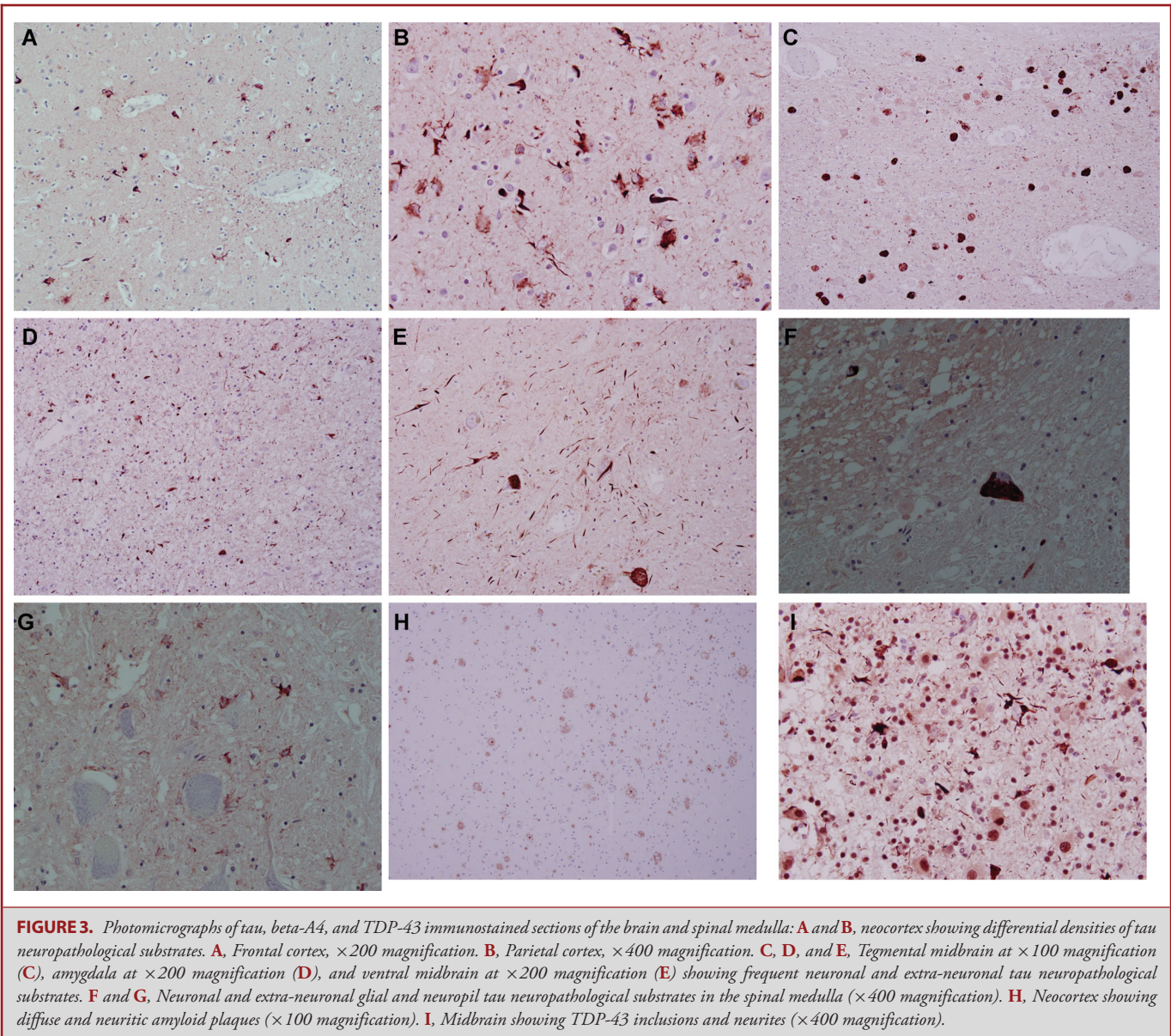


Selectively vulnerable regions of the brain may differentially manifest the neuropathological substrates of CTE earlier, and in greater quantities per unit volume and surface area, as the disease advances to the late stages when the brain globally manifests these neuropathological substrates. Some of these selectively vulnerable topographic regions of the brain may include, but may not be limited to, the midbrain, pons, limbic structures, parasagittal, and periventricular regions of the brain.<sup>1,4,21,28</sup> These are the sagittal and parasagittal regions of the brain that appear to bear the maximal shearing, angular–rotational acceleration–deceleration forces in traumatic brain injuries and in American football players.<sup>29–31</sup> This pathology progression involves neuronal circuits that are consistent with the selective and differential clinical symptomatology of CTE, predominantly mood and behavioral symptoms in younger patients, progressing to increasing cognitive deficits, and, eventually, dementia in older patients with advanced stages of CTE<sup>32</sup> as the neocortex becomes globally involved.

Our brain autopsy showed differential distribution of tau and amyloid neuropathological CTE substrates in the bilateral neocortex in a dorsal–ventral gradient, as was observed with [F-18]FDDNP-PET (Figure 1).<sup>1,4</sup> A limitation of this work, however, is the 52-mo interval between the [F-18]FDDNP-PET

brain imaging and brain autopsy. Since CTE is a progressive disease, further progression of neuropathological substrates should have existed over this period. This is particularly evident in this case, when the subject was diagnosed with motor neuron disease 2 yr after PET scanning, and suffered advancing symptoms until death. In spite of this temporal limitation, remnants of the differential lobar neocortical distribution of tau and amyloid neuropathological substrates were still observed at autopsy. The frontal, temporal, and parietal cortices, at autopsy, revealed uniformly high distribution and densities of neuropathological substrates, while the occipital cortex revealed lower densities (Table 5). Clinical dementia ratings performed several years prior to death can accurately predict postmortem regional and topographically selective neuropathology.<sup>33,34</sup> Unfortunately, the spinal cord was not included in the [F-18]FDDNP-PET scanning, since the patient was not manifesting any motor symptoms of CTME at the time of the scanning.

The lack of statistical correlation between our TDP-43 neuropathological findings and [F-18]FDDNP DVRs in this case, as well as the lack of correlation with amyloid deposition, may indicate that the [F-18]FDDNP-PET brain signal, in this case, originated principally in the presence of tau neuroaggregates (Figure 2). As has been previously suggested, the



TDP-43 inclusion bodies did not show any amyloid fibrillary structures within them<sup>1,35</sup> and in vivo [F-18]FDDNP signal was less likely to have significantly originated from these inclusions.

Our prior research<sup>1,4</sup> and current findings are indicating that [F-18]FDDNP-PET brain imaging may be a useful in vivo radiological tool for the clinical assessment and diagnosis of traumatic encephalopathy syndromes<sup>6</sup> including CTE, CTME, and CTE-PTSD (post-traumatic stress disorder). Further evaluation with clinical trials is warranted. Subconcussion and concussion based CTE may be differentially selective of the regions of the brain that bear the maximal shearing, angular-rotational acceleration-

deceleration forces<sup>29-31</sup> (parasagittal and periventricular regions and nuclei of the brain), progressing in topographic distribution to recruit more neocortical and subcortical regions as the disease advances. This may explain the progressive nature of the clinical symptoms and their correlation with deteriorating neuronal circuits.<sup>1,4</sup> Further studies are needed to confirm this progressive pathology model in living subjects.

## CONCLUSION

In conclusion, our results may suggest that the in vivo identification of CTE substrates in living patients may not only be

based on the presence or absence of proteinopathies, but also on the identification of the differential and selective topographic vulnerability unique to CTE, which [F-18]FDDNP-PET may be demonstrating. Further prospective studies are needed to assess whether [F18]FDDNP PET can serve as a useful adjunct in the diagnosis of CTE in living patients.

## Disclosures

Dr Omalu, Dr Barrio, Dr Small, Dr Huang, Dr Satyamurthy, and Mr Fitzsimmons JD are members of TauMark LLC, a limited liability company that owns the licensing rights to [F-18]FDDNP-PET technology. The other authors have no personal, financial, or institutional interest in any of the drugs, materials, or devices described in this article. Funding was received from the National Institutes of Health (P01-AG025831 and M01-RR00865), the Toulmin Foundation, Sheridan Lorenz, and Robert and Marion Wilson. No company provided research funding for this study. Dr Omalu, Dr Bailes, Ms Hammers, DO, and Mr Fitzsimmons, JD are directors of Brain Injury Research Institute, Inc (BIRI), which is a 501c3 charitable/research company that performs brain autopsies and analysis including Chronic Traumatic Encephalopathy (CTE) diagnosis. No director has received any compensation from BIRI for any work performed or otherwise. Mr Fitzsimmons has not represented any client that alleged a diagnosis of CTE or defended a claim disputing CTE.

## REFERENCES

- Barrio JR, Small GW, Wong KP, et al. In vivo characterization of chronic traumatic encephalopathy using [F-18]FDDNP PET brain imaging. *Proc Natl Acad Sci USA*. 2015;112(16):E2039-E2047.
- Shoghi-Jadid K, Small GW, Agdeppa ED, et al. Localization of neurofibrillary tangles and beta-amyloid plaques in the brains of living patients with Alzheimer disease. *Am J Geriatr Psychiatry*. 2002;10(1):24-35.
- Jacobson A, Petric A, Hogenkamp D, Sinur A, Barrio JR. 1,1-dicyano-2-1-[dimethylamino]naphthalen-2-yl]propene (DDNP): a solvent polarity and viscosity sensitive fluorophore for fluorescence microscopy. *J Am Chem Soc*. 1996;118:5572-5579.
- Small GW, Kepe V, Siddarth P, et al. PET scanning of brain tau in retired national football league players: preliminary findings. *Am J Geriatr Psychiatry*. 2013;21(2):138-144.
- Greenfield JG, Graham DI, Lantos PL. *Greenfield's Neuropathology*. 7th ed. London; New York: Arnold; 2002.
- Reams N, Eckner JT, Almeida AA, et al. A clinical approach to the diagnosis of traumatic encephalopathy syndrome: a review. *JAMA Neurol*. 2016;73(6):743-749.
- Folstein MF, Folstein SE, McHugh PR. "Mini-mental state". A practical method for grading the cognitive state of patients for the clinician. *J Psychiatr Res*. 1975;12(3):189-198.
- Lezak MD, Howieson DB, Loring DW. *Neuropsychological Assessment*. 4th ed. Oxford; New York: Oxford University Press; 2004.
- Liu J, Kepe V, Zabjek A, et al. High-yield, automated radiosynthesis of 2-(1-[6-[(2-[18F]fluoroethyl)(methyl)amino]-2-naphthyl]ethylidene)malononitrile ([18F]FDDNP) ready for animal or human administration. *Mol Imaging Biol*. 2007;9(1):6-16.
- US Pharmacopeial Convention. *Positron Emission Tomography Drugs for Compounding, Investigational, and Research Uses. US Pharmacopeia 36—National Formulary 31, General Chapter 823*. Rockville, MD: US Pharmacopeial Convention; 2013.
- Small GW, Kepe V, Ercoli LM, et al. PET of brain amyloid and tau in mild cognitive impairment. *N Engl J Med*. 2006;355(25):2652-2663.
- Kepe V, Huang SC, Small GW, Satyamurthy N, Barrio JR. Visualizing pathology deposits in the living brain of patients with Alzheimer's disease. *Methods Enzymol*. 2006;412:144-160.
- Tantawy MN, Jones CK, Baldwin RM, et al. [(18F)]Fallypride dopamine D2 receptor studies using delayed microPET scans and a modified Logan plot. *Nucl Med Biol*. 2009;36(8):931-940.

- Mirra SS, Heyman A, McKeel D, et al. The Consortium to Establish a Registry for Alzheimer's Disease (CERAD). Part II. Standardization of the neuropathologic assessment of Alzheimer's disease. *Neurology*. 1991;41(4):479-486.
- Benjamini Y, Hochberg Y. Controlling the false discovery rate: a practical and powerful approach to multiple testing. *J R Statist Soc B*. 1995;57(1):289-300.
- Ling H, Holton JL, Shaw K, Davey K, Lashley T, Revesz T. Histological evidence of chronic traumatic encephalopathy in a large series of neurodegenerative diseases. *Acta Neuropathol*. 2015;130(6):891-893.
- McKee AC, Cairns NJ, Dickson DW, et al. The first NINDS/NIBIB consensus meeting to define neuropathological criteria for the diagnosis of chronic traumatic encephalopathy. *Acta Neuropathol*. 2016;131(1):75-86.
- Crary JF, Trojanowski JQ, Schneider JA, et al. Primary age-related tauopathy (PART): a common pathology associated with human aging. *Acta Neuropathol*. 2014;128(6):755-766.
- Kovacs GG, Ferrer I, Grinberg LT, et al. Aging-related tau astroglialopathy (ARTAG): harmonized evaluation strategy. *Acta Neuropathol*. 2016;131(1):87-102.
- Omalu B, Bailes J, Hamilton RL, et al. Emerging histomorphologic phenotypes of chronic traumatic encephalopathy in American athletes. *Neurosurgery*. 2011;69(1):173-183; discussion 183.
- Omalu BI, DeKosky ST, Hamilton RL, et al. Chronic traumatic encephalopathy in a national football league player: part II. *Neurosurgery*. 2006;59(5):1086-1092; discussion 1092-1093.
- McKee AC, Stern RA, Nowinski CJ, et al. The spectrum of disease in chronic traumatic encephalopathy. *Brain*. 2013;136(Pt 1):43-64.
- McKee AC, Gavett BE, Stern RA, et al. TDP-43 proteinopathy and motor neuron disease in chronic traumatic encephalopathy. *J Neuropathol Exp Neurol*. 2010;69(9):918-929.
- Armstrong RA, McKee AC, Stein TD, Alvarez VE, Cairns NJ. A quantitative study of tau pathology in eleven cases of chronic traumatic encephalopathy. *Neuropathol Appl Neurobiol*. 2016;43(2):154-166. PMID: 26998921
- Smid LM, Kepe V, Vinters HV, et al. Postmortem 3-D brain hemisphere cortical tau and amyloid- $\beta$  pathology mapping and quantification as a validation method of neuropathology imaging. *J Alzheimers Dis*. 2013;36(2):261-274. PMID: 23568102
- Omalu BI, DeKosky ST, Minster RL, Kamboh MI, Hamilton RL, Wecht CH. Chronic traumatic encephalopathy in a National Football League player. *Neurosurgery*. 2005;57(1):128-134; discussion 128-134.
- McKee AC, Stein TD, Kiernan PT, Alvarez VE. The neuropathology of chronic traumatic encephalopathy. *Brain Pathol*. 2015;25(3):350-364.
- McKee AC, Cantu RC, Nowinski CJ, et al. Chronic traumatic encephalopathy in athletes: progressive tauopathy after repetitive head injury. *J Neuropathol Exp Neurol*. 2009;68(7):709-735.
- Ropper AH, Gorson KC. Clinical practice. Concussion. *N Engl J Med*. 2007;356(2):166-172.
- Bailes JE, Petraglia AL, Omalu BI, Nauman E, Talavage T. Role of subconcussion in repetitive mild traumatic brain injury. *J Neurosurg*. 2013;119(5):1235-1245.
- McAllister TW. Neurobiological consequences of traumatic brain injury. *Dialogues Clin Neurosci*. 2011;13(3):287-300. PMID: 22033563
- Stern RA, Daneshvar DH, Baugh CM, et al. Clinical presentation of chronic traumatic encephalopathy. *Neurology*. 2013;81(13):1122-1129.
- Schnaider Beeri M, Silverman JM, Schmeidler J, et al. Clinical dementia rating performed several years prior to death predicts regional Alzheimer's neuropathology. *Dement Geriatr Cogn Disord*. 2008;25(5):392-398.
- Clark CM, Pontecorvo MJ, Beach TG, et al. Cerebral PET with florbetapir compared with neuropathology at autopsy for detection of neuritic amyloid- $\beta$  plaques: a prospective cohort study. *Lancet Neurol*. 2012;11(8):669-678.
- Robinson JL, Geser F, Stieber A, et al. TDP-43 skeins show properties of amyloid in a subset of ALS cases. *Acta Neuropathol*. 2013;125(1):121-131.

---

**Neurosurgery Speaks!** Audio abstracts available for this article at [www.neurosurgery-online.com](http://www.neurosurgery-online.com).

---

## Acknowledgments

We are extremely grateful to the patient's family for their invaluable support and co-operation, without that this work would not be possible. We thank Natacha Donoghue and Jacqueline Martinez for subject scheduling and management; John Williams, University of California, Los Angeles, Nuclear Medicine Clinic, for performing the PET scans; Vladimir Kepe, Cleveland Clinic, for developing the [F-18]FDDNP-PET analysis procedures for proteinopathies in patients with neurodegenerative diseases, including CTE; and Billy West and Bus Cook for guidance with subject referral and for their helpful input. Funding from the National Institutes of Health (P01-AG025831 and M01-RR00865), the Toulmin Foundation, Sheridan Lorenz and Robert and Marion Wilson is highly appreciated.

## COMMENT

**T**his manuscript describes an in vivo PET technique which may help monitor the development of CTE and allow better correlation of symptoms with evolving pathology. As we strive to better understand the link between repetitive mTBI and neurodegeneration, and to better understand the the clinical correlate of the pathologic entity CTE, such in vivo techniques are critical. The manuscript is clearly limited with  $n = 1$ , but hopefully shows a potential in vivo way of helping to better define this rare condition.

**Colin Smith**

*Edinburgh, United Kingdom*